Journal of Alloys and Compounds 656 (2016) 871–875

Contents lists available at ScienceDirect

Journal of Alloys and Compounds

journal homepage: http://www.elsevier.com/locate/jalcom

Ferroelectric polarizing-induced non-volatile modulation effect on magnetic properties and its Raman detection in Ni/PMN-PT heterostructure

S.Y. Chen [a, b, *], H.Q. Zhang [a], Q.Y. Ye [a], Z.Q. Hu [b], Z.G. Huang [a], N.X. Sun [b]

[a] College of Physics and Energy, Fujian Provincial Key Laboratory of Quantum Manipulation and New Energy Materials, Fujian Normal University, Fuzhou, 350108, China
[b] Department of Electrical and Computer Engineering, Northeastern University, Boston, MA, 02115, USA

ARTICLE INFO

Article history:
Received 11 August 2015
Received in revised form
30 September 2015
Accepted 6 October 2015
Available online 14 October 2015

Keywords:
Magnetoelectric heterostructure
Magnetic properties
Electric field
Non-volatile modulation effect

ABSTRACT

In situ tuning effect on magnetism is often achieved by electric-field-induced inverse piezoelectric effect in ferromagnetic/piezoelectric structures. Here, we report on a non-volatile tuning of magnetic properties in Ni/Pb($Mg_{1/3}Nb_{2/3}$)O_3–$PbTiO_3$ heterostructure. Both magnetization difference of up to 60% and coercivity difference of up to 23.2% are obtained by electric-field-induced the change of polar state in the substrate. This modulation effect is observed over a broad range of temperatures. The coincident changes of both magnetic properties and Raman scattering spectra with different polarization times for the heterostructure are detected, which indicates that the non-volatile tuning effect on magnetism is attributed to the change of the magnetic anisotropy result from the ferroelectric polarizing induced-strain.

Recently, electric (E)-field-manipulated magnetic properties in magnetoelectric (ME) systems have received much attention for their potential applications and intriguing physical properties [1–7]. A framework for creating novel functionalities has been achieved in ferromagnetic/ferroelectric (FM/FE) heterostructures, which bases on electrically tunable magnetic properties through strain-mediated ME coupling [1,5,7–13], such as ferromagnetic resonance tuning [14–16], magnetization (M) and coercivity (H_c) tuning in magnetic thin film [2,17–23] and magnetic islands [24–26]. Most of these investigations mainly focused on *in situ* tuning, i.e., in FM/FE heterostructures, magnetic or electric properties of FM phases were simultaneously measured when E-field was *in situ* applied to FE phase [2–4,12–14,17–23,27,28]. This *in situ* tuning of magnetism is volatile because the piezoelectric-induced strain can decay after E-field is removed from FE phase. To date, non-volatile modulation of magnetic state by using strain was still far from being fully explored. And most of the reports have not clearly demonstrated the non-volatility of the modulation effect on magnetic properties by E-field in different external conditions [3,15,21,29,30]. In this paper, the magnetic properties modulated by E-field-induced FE polarizing in Ni/0.71Pb($Mg_{1/3}Nb_{2/3}$)O_3–0.29$PbTiO_3$ (001) (named as Ni/PMN-PT) heterostructure were investigated in detail. Obvious non-volatile tuning of both M and H_c was obtained. And Raman scattering spectra (*Rss*) was proposed to detect the FE polarizing-induced strain in PMN-PT substrate, which contributes to non-volatile modulation effect of E-field on the magnetic properties in Ni/PMN-PT heterostructure.

Ferromagnetic Ni thin film was deposited on the (001)-oriented PMN-PT single-crystal substrate by pulsed laser deposition (PLD) method using a KrF excimer laser ($\lambda = 248$ nm). The base pressure of the chamber was below 3×10^{-7} torr. The energy of the laser beam was 400 mJ, and the repetition rate was 4 Hz. During deposition, the substrate temperature was kept at 300 K. The upper left inset of Fig. 1 presents the schematic of the Ni/PMN-PT heterostructure. The thickness of Ni thin film is 60 nm. The crystal structure of the film was examined using X-ray diffraction. Raman spectrometer (LabRAM HR Evolution, Jobin Yvon Co., Longjumeau, France) with laser wavelength of 532 nm was used to detect the *Rss* of PMN-PT. Magnetic measurements were performed using a vibrating sample magnetometer (VersLab-VSM, Quantum Design Co., San Diego, CA, USA). The direction of E-field is along <001>

* Corresponding author. College of Physics and Energy, Fujian Provincial Key Laboratory of Quantum Manipulation and New Energy Materials, Fujian Normal University, Fuzhou, 350108, China.
E-mail address: sychen@fjnu.edu.cn (S.Y. Chen).

http://dx.doi.org/10.1016/j.jallcom.2015.10.056
0925-8388/

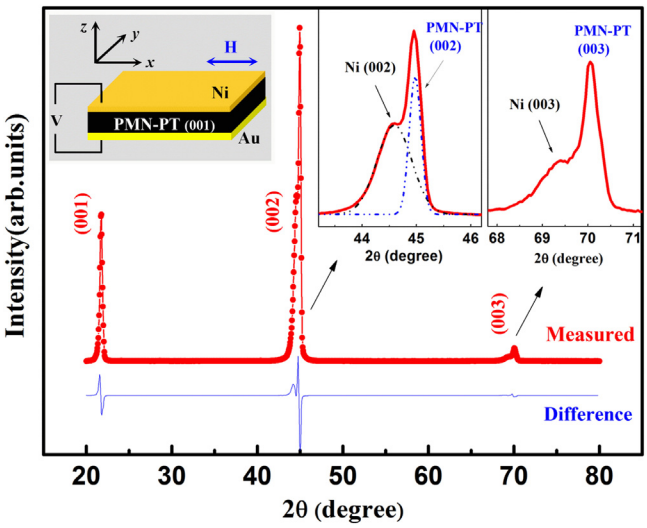

Fig. 1. The x-ray diffraction patterns of Ni/PMN-PT heterostructure. The upper left inset shows the structure schematic of the sample. The upper right insets present the enlarged image of XRD pattern near 44.5 and 69.5°, respectively.

direction of the PMN-PT substrate. And the direction of external magnetic field (H) is parallel to the Ni thin film.

The x-ray diffraction pattern of Ni/PMN-PT heterostructure is shown in Fig. 1. Three obvious diffraction peaks of the PMN-PT single crystal substrate can be indexed. The upper right insets of the figure present enlarged local images of the XRD patterns. Obviously, (002) and (003) diffraction peaks of the substrate are both accompanied by a small peak, respectively, suggesting the single phase and highly (001) - oriented epitaxial growth of the Ni film on the PMN-PT substrate.

The converse ME effect of the Ni/PMN-PT film was investigated by measuring magnetic hysteresis loops and thermomagnetic curves when applying different E-fields to the substrate. Here, we note that, before performing each magnetic measurement, an E-field is applied to the substrate for a pre-set time (i.e., polarization time, t_P) and then is turned off. We refer to this E-field as *ex situ* E-field (named as E_{ex}) to distinguish it from *in situ* measurements, where E-field is not turned off during ongoing magnetic and other properties measurements. [3,4,22,23] Typical M–H curves with different E_{ex} [Fig. 2(a)] show that, magnetic parameters, such as M and H_c, can be well modulated. In most cases concerning the strain-medium converse ME effect in FM/FE heterostructures, E-field was applied *in situ* to FE substrates, and linear reverse piezoelectric (*RPE*) effect was considered as the reason of producing converse ME effect [13,30,31]. This *in situ* tuning of the magnetic properties disappeared when E-field decreased to zero [31]. In this cases, the strain was induced by *RPE* effect. As we know, strain can also be induced by the distortion of FE phases during polarizing. In our case, the tuning effect of the E_{ex} on magnetic properties should be attributed to the strain induced by FE polarizing. The initial polar state of the PMN-PT is P_r^0 (equals to zero) in our sample. When suffered an E_{ex} (for example, 1 kV/cm) along <001> direction, the PMN-PT substrate is in a polarized state, and produces an in-plane strain, which may change the magnetic anisotropy of a magnetic thin film via magnetoelastic effect in FM/FE heterostructures [13,17]. This magnetoelastic effect can be described by the magnetoelastic energy (E_{me}), which contributes to the magnetic free energy (E_{tot}) of a magnetic material. And E_{tot} can be expressed as,

$$E_{tot} = E_0 + E_{me}, \tag{1}$$

where E_0 includes the exchange energy, Zeeman energy, demagnetization energy, and magneto-crystalline energy. The magnetoelastic energy, E_{me}, describes the effect of the strain on the magnetic anisotropy, and can be denoted as

$$E_{me} \propto -\frac{3}{2}\lambda_s \sigma \cos^2\theta, \tag{2}$$

where λ_s is magnetostrictive constant, θ is the angle between magnetization (M) and stress (σ). Therefore, the strain can change the magnetic free energy according to the above equations, and consequently change the magnetization which is dominated by a local minimum of E_{tot} in equilibrium.

From Fig. 2 (a), it can be seen that H_c of the Ni film also changes with E_{ex}. The strain makes the easy-axis (EA) of Ni thin film deviate from original direction and hence changes the magnetic anisotropy of the film, in other words, the strain produces an additional anisotropy (represented by an 'extrinsic' EA) in the film [32]. Therefore, if we want to reduce the remnant magnetization (M_r) to zero, we should apply an additional reverse H to the sample to overcome the additional magnetic anisotropy. Consequently, H_c of the sample increases [32]. If we define H_c difference as $\Delta H_c/H_c(0) = [H_c(E_{ex}) - H_c(0)]/H_c(0))$, up to 23.2% of the H_c difference value is obtained when applying an E_{ex} (= 2 kV/cm) to the PMN-PT.

Next, we consider the modulation effect of E_{ex} on magnetization in different magnetic states (under different H). Here, we define magnetization difference as $\Delta M/M_s = [M(E_{ex}) - M]/M_s$, where $M_s(0)$ is the saturation magnetization of Ni film of the sample. According to Fig. 2 (a), we can calculate the values of $\Delta M/M_s$ in different H. Fig. 2 (b) shows the $\Delta M/M_s$ –H curve with $E_{ex} = 3$ kV/cm. From the figure, It can be concluded that, (1) FE polarizing-assisted magnetization process exists in the measured H region. (2) $\Delta M/M_s$ is obviously enhanced near $H_c(0)$, a large value of up to 60% is obtained at H = 56 Oe. (3) at zero H, the value of $\Delta M/M_s$ is still up to 26%, which implies that FE polarizing-induced magnetic anisotropy can also be achieved when lacking of an external magnetic field. Besides, it is noticed from the inset of Fig. 2 (a) that, although M_r can be changed markedly by E_{ex}, the values of M_s with different E_{ex} are almost the same. This result is similar to that in other ME heterostructures [18,29], and suggests that E_{ex} applied on the substrate can only change the magnetic anisotropy of Ni film, and has no obvious effect on the intrinsic magnetization.

To further understand the relation between M and E_{ex} in zero H, we present the E_{ex} dependence of M_r for the Ni/PMN-PT, as shown in Fig. 3(a). It can be seen that M_r changes rapidly with E_{ex} increasing up to near the coercive field (E_c) of PMN-PT ($E_c = 2.9$ kV/cm). E_{ex} further increasing does not lead to obvious change of M_r. As we know, PMN-PT reaches saturation polarization when E_{ex} is slightly larger than E_c. Therefore, in $E_{ex} > E_c$ region, E_{ex} further increasing cannot change remnant polarization of PMN-PT, which means that Ni film is in the same strain state, and M_r does not change obviously in with E_{ex} further increasing. From Fig. 3(a), the value of M_r difference ($\Delta M_r/M_r(0)$, defined as $[M_r(E) - M_r(0)]/M_r(0)$) up to 50.1% is obtained when $E_{ex} = 3$ kV/cm, indicating large non-volatile modulation effect of E_{ex} on the magnetism at zero external H.

To investigate the temperature (T) stability about modulation effect on magnetic properties, we performed measurements of the modulation effect at different T. Fig. 3(b) shows the T dependence of M_r for the Ni film when PMN-PT substrate is in different polar states. The dash line presents the M_r–T relation with zero electric field. In the measurement, when T increases up to 212 K, we change the polar state of the substrate by applying an E_{ex} of 1.5 kV/cm. It is found that M_r jumps markedly to another value, and continues to decrease smoothly with T increasing. Once again, M_r jumps to a higher value when a higher E_{ex} (4.0 kV/cm) is applied to the PMN-

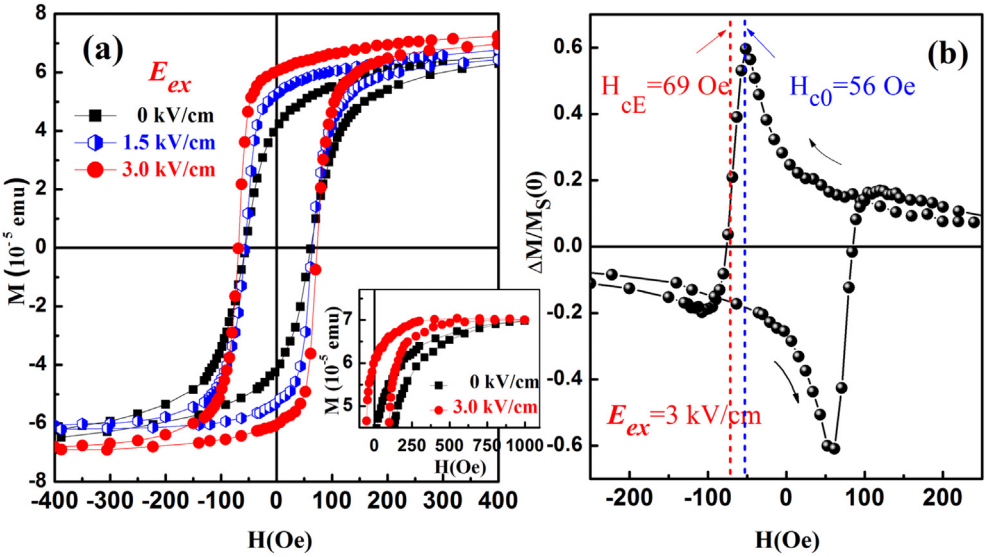

Fig. 2. Typical M–H loops with different E_{ex} (a) and $\Delta M/M_s(0)$ as a function of H with an E_{ex} of 3 kV/cm (b) for Ni/PMN-PT. The inset shows the M–H curves in the H region between 0 and 1 kOe.

PT at 267 K. The calculated $\Delta M_r/M_r(0)$ is up to 60.1% at 150 K. This value reduces to about 40% at 320 K. The results indicate that obvious non-volatile modulation effect on magnetization in Ni/PMN-PT heterostructure exists over broad temperature region.

As is well-known, it takes time to complete the FE polarizing process. At certain value of E_{ex}, different polarization times (t_p) may produce different polar states in FE phase, and therefore changes the magnetic states of FM phase now that the tuning of magnetism is attributed to the FE polarizing-induced strain in the FE phase. To confirm this issue, we performed magnetic properties measurements after PMN-PT had been polarized by an E_{ex} for different t_p. The detail processes of the measurements are as following. After an E_{ex} is applied to the PMN-PT substrate for a set t_p, M–H loop of the Ni film was measured. Then, t_p is increased and the substrate is polarized again. And another M–H loop was measured. The above measurement processes are repeated for several times by changing t_p. Thus, we can obtain the relation between H_c and t_p. Fig. 3 shows the dependence of H_c on t_p when applying E_{ex} of 4 kV/cm and 8 kV/cm to the substrate, respectively. It can be seen that, for certain E_{ex}, different t_p markedly influences H_c of the Ni film. We first consider the case with $E_{ex} = 4$ kV/cm (Fig. 3(a)). When t_p increases from zero to about 5 min, H_c increases gradually, indicating that short t_p makes no obvious change in H_c. Further increasing in t_p induces a sharp increase in H_c, which may correspond to an obvious FE polarizing in PMN-PT. When t_p is sufficiently long, this FE polarizing terminates, resulting in a relative stable H_c. Distinctively, in the case with $E_{ex} = 8$ kV/cm, much shorter t_p is needed to make H_c increase and reach stable value, as can be seen in Fig. 3(b). The reason should be that, larger E-field strength is more easily to drive FE polarizing. Besides, the change of M_r with different t_p is also considered. The insets of Fig. 3(a) and (b) present M_r–t_p curves for the sample when E_{ex} equals to 4 kV/cm and 8 kV/cm, respectively. It is observed that, there are similar change relations between H_c– t_p curve and M_r–t_p curve under the same E_{ex}, i.e., when t_p increases, the changes of both M_r and H_c are synchronous and consistent. These results indicate a correlation between the polar state of FE phase and the magnetism of FM phase in Ni/PNM-PT heterostructure.

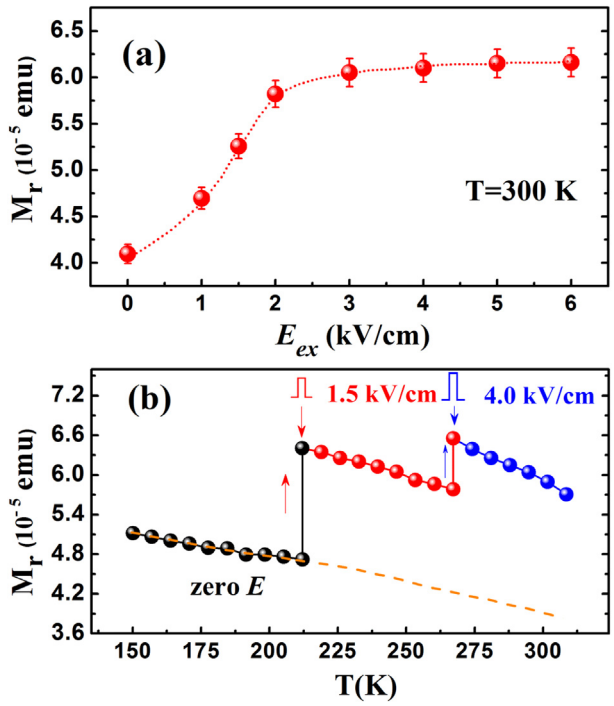

Fig. 3. E_{ex} dependence of M_r at room temperature (a) and M_r–T curve with different E_{ex} (b) for Ni/PMN-PT. The dash orange line presents the M_r–T curve within whole measured temperature region under $E_{ex} = 0$. (For interpretation of the references to colour in this figure legend, the reader is referred to the web version of this article.)

Raman scattering is very sensitive to the strain state and tiny shift in materials. Therefore, we can use *Rss* to detect the changes of the shape and strain when PMN-PT is polarized for different t_p. The schematic of the *Rss* measurements for Ni/PMN-PT is shown in Fig. 5(a1), in which the laser is applied to the PMN-PT along -*y* direction, and E_{ex} is applied along <001> direction (*z* direction). When PMN-PT is in non-polarized state ($P_r = 0$), the laser is accurately focused on the surface of the PMN-PT by tuning the objective lens in the Raman device, as shown in Fig. 5(a1). Then, *Rss* of the PMN-PT is measured. The result is shown in the top line of Fig. 5(b). Continually, several *Rss* were measured when PMN-PT is

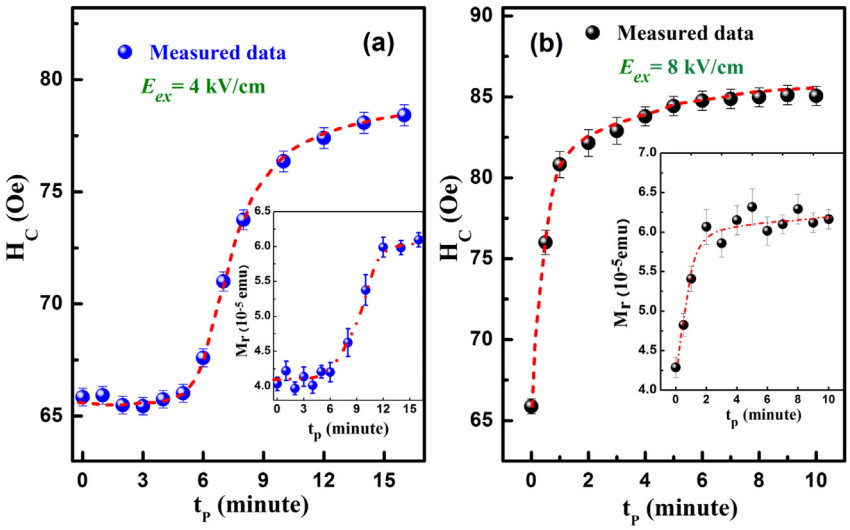

Fig. 4. t_p dependence of both H_c and M_r for Ni/PMN-PT. (a) E_{ex} = 4 kV/cm. (b) E_{ex} = 8 kV/cm. The dash lines in the figures are for visual guide.

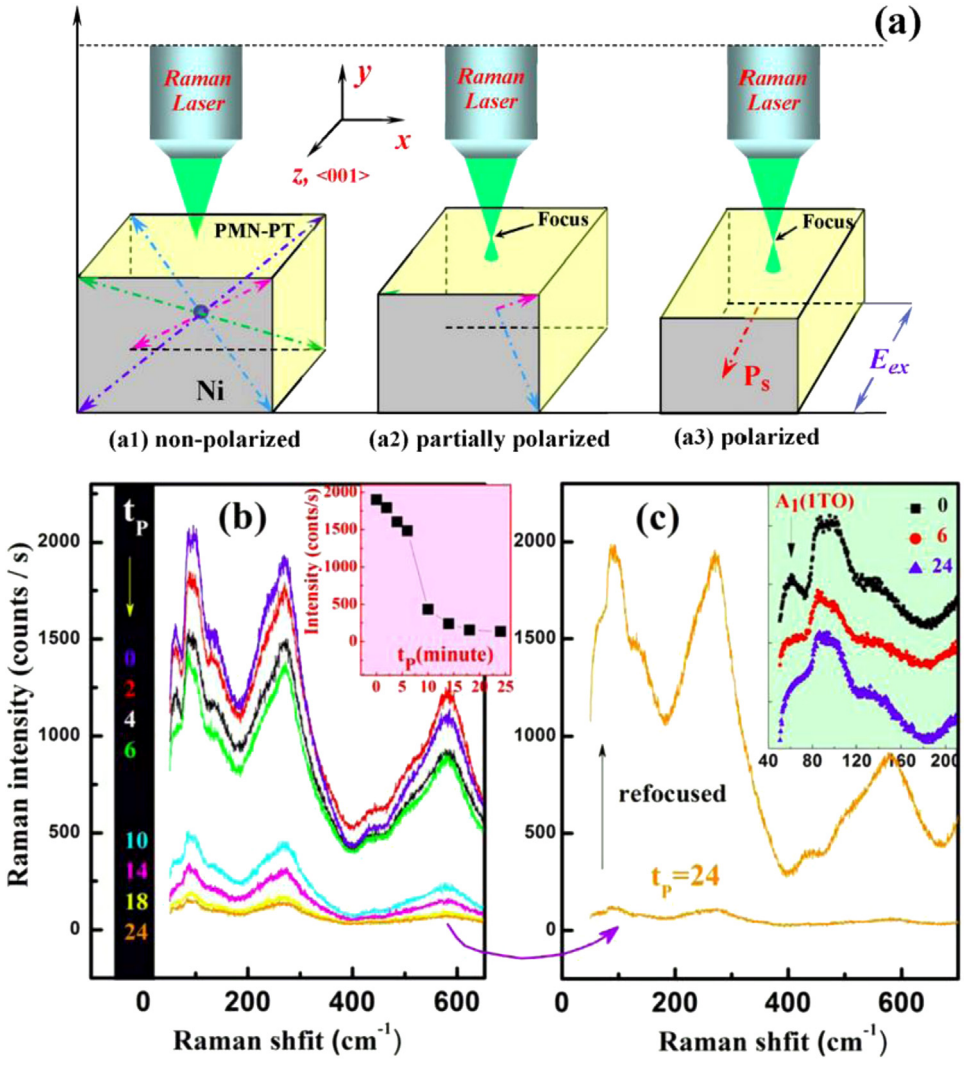

Fig. 5. (a) The schematic illustrations of *Rss* measurements for Ni/PMN-PT. Figures from (a1) to (a3) also present schematically the laser focus deviating from the surface of PMN-PT when PMN-PT is in different polar states. (b) *Rss* of the PMN-PT with different t_p. The inset presents typical relation between *Rss* intensity and t_p. (c) *Rss* with t_p = 24 min before and after readjusting the laser focus. The inset shows the change in Raman vibration mode (A_1(1TO)) with different t_p.

polarized by an E_{ex} of 4 kV/cm for different t_p. The results are also shown in Fig. 5(b). It is seen from the *Rss* with $t_P = 0$, three obvious Raman peaks can be indexed near 580, 270, and 60 cm^{-1}, which are the characteristic peaks of PMN-PT corresponding to the oxygen bending vibration, B-site ion against O stretching vibration inside the octahedra, and Pb against BO_6 octahedra translational vibration, respectively [33]. Next, we consider the changes of *Rss*. Firstly, we analyze *Rss* intensity of the sample polarized for different t_p. It can be seen that, when $t_P = 0$, *Rss* intensity is the strongest, and then decreases with t_P increasing. This decrease is more obvious when t_p changes from 6 to 14 min, as can be seen from the inset of Fig. 5(b), which presents the typical relation between *Rss* intensity and t_P. Here, the *Rss* intensity corresponds to the Raman peak located at 86 cm^{-1} in Fig. 5(b). When t_p is larger than 18 min, *Rss* intensity becomes very small. For further understanding, Fig. 5(a1), (a2) and (a3) present the schematic illustrations of this changing process. When (001)-origined PMN-PT single crystal is polarized along <001> direction, polarization (P_i) may rotate toward <001> direction. And PMN-PT may compress along *xy* plane (in-plane of Ni film) and stretch along *z* direction, resulting in deformation of the PMN-PT. Therefore, the laser focus deviates from the surface of the PMN-PT (Fig. 5(a2)), leading to the decrease of *Rss* intensity. When t_p increases, *Rss* intensity decreases accordingly since the deformation of PMN-PT is more serious (Fig. 5(a3)). After having measured the last *Rss* with $t_P = 24$ min (the last line of Fig. 5(b)), we adjusted the objective lens of the Raman device to make the laser refocus on the surface of the PMN-PT, and *Rss* was measured once again. It is found from Fig. 5(c) that, *Rss* intensity recovered again after the laser was refocused. Therefore, the changes of *Rss* intensity with different t_P reflect the deformation of the PMN-PT. Secondly, we consider the changes of Raman vibration mode. It can be seen from the inset of Fig. 5(c) that, the Raman vibration mode near 61 cm^{-1} (corresponding to Pb against BO_6 octahedra translational vibration, named as A_1(1TO) mode [33]) shifts toward low frequency, i.e., the Raman peak shifts from 61 cm^{-1} to 52 cm^{-1} when t_p increases from zero to 24 min (frequency shift $\Delta f = 9$ cm^{-1}). And the mode degenerates slowly with t_p increasing. These results about *Rss* indicate that the microstructure of PMN-PT changes under different polar states. Thirdly, it is found from Fig. 4(a) and Fig. 5(b) that, both magnetic parameters (H_c, M_r) and *Rss* intensity have almost synchronous responses to t_p. The above experimental results confirm that the non-volatile tuning effect of E_{ex} on the magnetic properties is attributed to the strain induced by FE polarizing.

In summary, obvious non-volatile modulation of E_{ex} on magnetic properties had been obtained in Ni/PMN-PT heterostructure over a broad range of temperatures, including room temperature. *Rss* and magnetic properties of the sample were measured when PMN-PT is in different FE polar states by applying E_{ex} to the substrate for different t_P. *Rss* intensity, Raman vibration mode and magnetic parameters of the sample changed synchronously with t_P increasing. Their coincident changes indicate that the non-volatile tuning effect should be attributed to the change of the magnetic anisotropy, which result from the FE polarizing induced-strain.

Acknowledgment

This work was supported by National Basic Research Program of China (Grant No. 2011CBA00200), National Natural Science Foundation of China (Grant No. 11004031), Program for New Century Excellent Talents of Fujian Province (Grant No. JA12054) and Key Project of Fujian Provincial Education Department (Grant No. JA15100).

References

[1] C.W. Nan, M.I. Bichurin, S. Dong, D. Viehland, G. Srinivasan, J. Appl. Phys. 103 (2008) 031101.
[2] M. Weiler, A. Brandlmaier, S. Geprägs, M. Althammer, M. Opel, C. Bihler, H. Huebl, M.S. Brandt, R. Gross, S.T.B. Goennenwein, New J. Phys. 11 (2009) 013021.
[3] Y. Lee, Z.Q. Liu, J.T. Heron, J.D. Clarkson, J. Hong, C. Ko, M.D. Biegalski, U. Aschauer, S.L. Hsu, M.E. Nowakowski, J. Wu, H.M. Christen, S. Salahuddin, J.B. Bokor, N.A. Spaldin, D.G. Schlom, R. Ramesh, Nat. Commun. 6 (2015) 6959.
[4] J. Ma, J.M. Hu, Z. Li, C.W. Nan, Adv. Mater. 23 (2011) 1062.
[5] M. Liu, N.X. Sun, Philos. Trans. R. Soc. A 372 (2014) 20120439.
[6] H.Q. Shen, Y.G. Wang, D. Xie, J.H. Cheng, J. Alloy Compd. 610 (2014) 11.
[7] S. Fusil, V. Garcia, A. Barthelemy, M. Bibes, Annu. Rev. Mater. Res. 44 (2014) 91.
[8] S.H. Zhang, J.P. Zhou, Z. Shi, P. Liu, C.Y. Deng, J. Alloy Compd. 590 (2014) 46.
[9] J.F. Scott, Nat. Mater. 6 (2007) 256.
[10] Y.H. Chu, L.W. Martin, M.B. Holcomb, R. Ramesh, Mater. Today 10 (2007) 16.
[11] J.M. Hu, Z. Li, L.Q. Chen, C.-W. Nan, Nat. Commun. 2 (2011) 553.
[12] Y.J. Wang, J.F. Li, D. Viehland, Mater. Today 17 (2014) 269.
[13] A. Brandlmaier, S. Geprägs, M. Weiler, A. Boger, M. Opel, H. Huebl, C. Bihler, M.S. Brandt, B. Botters, D. Grundler, R. Gross, S.T.B. Goennenwein, Phys. Rev. B 77 (2008) 104445.
[14] M. Liu, O. Obi, J. Lou, Y.J. Chen, Z.H. Cai, S. Stoute, M. Espanol, M. Lew, X.D. Situ, K.S. Ziemer, V.G. Harris, N.X. Sun, Adv. Funct. Mater. 19 (2009) 1826.
[15] N.N. Phuoc, C.K. Ong, Appl. Phys. Lett. 105 (2014) 032901.
[16] J.M. Vargas, J. Gómez, APL Mater. 2 (2014) 106105.
[17] T. Wu, A. Bur, P. Zhao, K.P. Mohanchandra, K. Wong, K.L. Wang, C.S. Lynch, G.P. Carman, Appl. Phys. Lett. 98 (2011) 012504.
[18] Y.T. Yang, Q.M. Zhang, D.H. Wang, a) Y.Q. Song, L.Y. Wang, L.Y. Lv, Q.Q. Cao, Y.W. Du, Appl. Phys. Lett. 103 (2013) 082404.
[19] J.L. Hockel, A. Bur, T. Wu, K.P. Wetzlar, G.P. Carman, Appl. Phys. Lett. 100 (2012) 022401.
[20] D.R. Patil, R.C. Kambale, Y.S. Chai, W.H. Yoon, D.Y. Jeong, D.S. Park, J.W. Kim, J.J. Choi, C.W. Ahn, B.D. Hahn, S.J. Zhang, K.H. Kim, J. Ryu, Appl. Phys. Lett. 103 (2013) 052907.
[21] J.L. Hockel, S.D. Pollard, K.P. Wetzlar, T. Wu, Y. Zhu, G.P. Carman, Appl. Phys. Lett. 102 (2013) 242901.
[22] S. Cherepov, P.K. Amiri, J.G. Alzate, K. Wong, M. Lewis, P. Upadhyaya, J. Nath, M.Q. Bao, A. Bur, T. Wu, G.P. Carman, A. Khitun, K.L. Wang, Appl. Phys. Lett. 104 (2014) 082403.
[23] R.O. Cherifi, V. Ivanovskaya, L.C. Phillips, A. Zobelli, I.C. Infante, E. Jacquet, V. Garcia, S. Fusil, P.R. Briddon, N. Guiblin, A. Mougin, A.A. Ünal, F. Kronast, S. Valencia, B. Dkhil, A. Barthélémy, M. Bibes, Nat. Mater. 13 (2014) 345.
[24] J.L. Hockel, A. Bur, T. Wu, K.P. Wetzlar, G.P. Carman, Appl. Phys. Lett. 100 (2012) 022401.
[25] M. Buzzi, R.V. Chopdekar, J.L. Hockel, A. Bur, T. Wu, N. Pilet, P. Warnicke, G.P. Carman, L.J. Heyderman, F. Nolting, Phys. Rev. Lett. 111 (2013) 027204.
[26] J.Z. Cui, J.L. Hockel, P.K. Nordeen, D.M. Pisani, C.Y. Liang, G.P. Carman, C.S. Lynch, Appl. Phys. Lett. 103 (2013) 232905.
[27] Z.G. Wang, Y. Zhang, Y.J. Wang, Y.X. Li, H.S. Luo, Jiefang Li, D. Viehland, ACS Nano 8 (2014) 7793.
[28] W.P. Zhou, Q. Li, Y.Q. Xiong, Q.M. Zhang, D.H. Wang, Q.Q. Cao, L.Y. Lv, Y.W. Du, Sci. Rep. 4 (2014) 699.
[29] S.W. Yang, R.C. Peng, T. Jiang, Y.K. Liu, L. Feng, J.J. Wang, L.Q. Chen, X.G. Li, C.W. Nan, Adv. Mater. 26 (2014) 7091.
[30] T.X. Nan, M. Liu, W. Ren, Z.G. Ye, N.X. Sun, Sci. Rep. 4 (2014) 5931.
[31] C.J. Hsu, J.L. Hockel, G.P. Carman, Appl. Phys. Lett. 100 (2012) 092902.
[32] L. Callegaro, E. Puppin, Appl. Phys. Lett. 68 (1996) 1279.
[33] M.R. Shen, G.G. Siu, Z.K. Xu, W.W. Cao, Appl. Phys. Lett. 86 (2005) 252903.